

Roles of Electron Correlations in the Spin-Triplet Superconductivity of Sr_2RuO_4

Takuji NOMURA and Kosaku Yamada

Department of Physics, Kyoto University, Kyoto, 606-8502, Japan

(Received)

We discuss a microscopic mechanism of the spin-triplet superconductivity in the quasi-two-dimensional ruthenium oxide Sr_2RuO_4 on the basis of two-dimensional three-band Hubbard model. We solve the linearized Éliashberg equation by taking into account the full momentum-frequency dependence of the order parameter for the spin-triplet and the spin-singlet states, and estimate the transition temperature as a function of the Coulomb integrals. The effective pairing interaction is expanded perturbatively with respect to the Coulomb interaction at the Ru sites up to the third order. As a result, we show that the spin-triplet p -wave state is more stable than the spin-singlet d -wave state for moderately strong Coulomb interaction. Our results suggest that one of the three bands, γ , plays a dominant role in the superconducting transition, and the pairing on the other two bands (α and β) is induced passively through the inter-orbit couplings. The most significant momentum dependence for the p -wave pairing originates from the vertex correction terms, while the incommensurate antiferromagnetic spin fluctuations, which are observed in inelastic neutron scattering experiments, are expected to disturb the p -wave pairing by enhancing the d -wave pairing. Therefore we can regard the spin-triplet superconductivity in Sr_2RuO_4 as one of the natural results of the electron correlations, but cannot consider as a result of some strong magnetic fluctuations. We will also mention the normal Fermi liquid properties of Sr_2RuO_4 .

KEYWORDS: electron correlations, three-band Hubbard model, third order perturbation theory, vertex corrections, Sr_2RuO_4 , spin-triplet superconductivity, superconducting transition temperature.

§1. Introduction

Clarifying the mechanism of the spin-triplet superconductivity in Sr_2RuO_4 has been one of the most challenging issues in the physics of strongly correlated electrons.^{1,2)} This unconventional pairing state has been accepted widely as a result of many intensive experimental and theoretical studies.

Some of the most remarkable results supporting the odd-parity parallel-spin pairing were obtained by the direct measurements of the spin susceptibility through the superconducting transition. The NMR Knight shift³⁾ and the inelastic polarized neutron⁴⁾ scattering measurements revealed that

the spin susceptibility of the electron system does not show any change at the transition. These facts indicate that the electron system does not lose all the activity in the spin space even in the superconducting phase, and exclude the possibility of the singlet Cooper pairing. In addition, there are many other observations suggesting indirectly but very strongly the realization of the unconventional pairing symmetry. The superconductivity is crucially destroyed by the slight concentration of nonmagnetic impurities,⁵⁾ in contrast to the conventional s -wave superconductivity. The NMR relaxation rate exhibits no coherence peak just below T_c .⁶⁾ The muon spin relaxation rate is increased below T_c , which indicates that an internal magnetic field is turned on spontaneously and the time-reversal symmetry breaks down in the superconducting state.⁷⁾ More recently there are several experiments reporting that the second superconducting phase transition occurs in the vicinity of H_{c2} curve.^{8,9)}

The normal state properties of Sr_2RuO_4 are quite different from those of high- T_c cuprates, in spite of the similarity in the crystal structures. Sr_2RuO_4 possesses a metallic conductivity without any carrier doping, and exhibits typical quasi-two-dimensional Fermi liquid behaviors, for example, the Pauli paramagnetism, the T^2 behavior in the resistivity at low temperatures.^{1,10)} The electronic structure is characterized by the three cylindrical Fermi surfaces, α , β and γ , according to the de Haas-van Alphen measurements.¹¹⁾ This is in good agreement with the results of the band structure calculations.^{12,13)}

From the theoretical point of view, Rice and Sigrist predicted the parallel-spin pairing shortly after the discovery of the superconductivity.¹⁴⁾ Their discussions are based on the facts that Sr_2RuO_4 gives a set of Fermi liquid parameters comparable to those of the superfluid ^3He and that the three-dimensional version SrRuO_3 is a ferromagnet. According to that situation, it seems quite natural to expect that some ferromagnetic spin fluctuations induce the spin-triplet superconductivity.^{15,16)} However the inelastic neutron scattering measurements did not detect any enhancement of ferromagnetic components but observed a sizeable incommensurate antiferromagnetic fluctuations in the spin susceptibility $\chi(q)$.¹⁷⁾ Therefore it is difficult to expect that some strong ferromagnetic fluctuations play the leading role for the superconductivity of Sr_2RuO_4 .

Here we would like to comment on some other theoretical considerations on the mechanism of the superconductivity. Some theorists consider that the observed incommensurate antiferromagnetic fluctuations mediate the superconductivity.^{18,19)} According to the discussions, the incommensurate fluctuations should possess a large anisotropy, $\chi_{zz}(Q_{\text{inc}}) > 2\chi_{-+}(Q_{\text{inc}})$. To our knowledge, however, such a high anisotropy has never been observed in Sr_2RuO_4 . Particularly, the recent neutron scattering measurement by Servant *et al.* suggests that the spin susceptibility $\chi(Q_{\text{inc}})$ is very isotropic.²⁰⁾ Recently magnetic properties of Ti-doped $\text{Sr}_2\text{Ru}_{1-x}\text{Ti}_x\text{O}_4$ have been investigated.²¹⁾ This compound exhibits the long range magnetic ordering for $x \geq 0.03$, which evolves from the incommensurate antiferromagnetic fluctuations. In the ordered phase, the spin moment

points along the c -axis direction.²²⁾ This anisotropy is qualitatively identical to that required in the anisotropic spin fluctuation scenario. What we should note here is, however, the following point. The effect of Ti-doping on the superconducting transition temperature is quite similar to that of other nonmagnetic impurity doping, in spite that the incommensurate fluctuations are much enhanced by Ti-doping.²³⁾ If the incommensurate fluctuations mediated the superconductivity, the transition temperature should behave for Ti-dopings in a different way from the case of other non-magnetic impurity doping. Consequently, we consider that the incommensurate antiferromagnetic fluctuations are not essential for the superconductivity of Sr_2RuO_4 .

A scenario based on the incommensurate orbital fluctuations was discussed.²⁴⁾ In order to explain the spin-triplet superconductivity, however, they require rather strong inter-orbit repulsion between $\text{Ru}4d\varepsilon$ electrons. The effect of the inter-orbit repulsion usually becomes weak remarkably by the screening. Therefore we consider that the incommensurate orbital fluctuations are not large enough to stabilize the spin-triplet pairing in Sr_2RuO_4 .

There are some other scenarios based on the Hund's coupling.^{25,26,27)} The Hund's coupling is usually attractive only for two parallel-spin particles which are in the different orbits on the same localized atom. Therefore it seems that the Hund's coupling does not necessarily play an important part for stabilizing the parallel spins over the coherence length. In addition, the hybridization among the atomic orbitals $\text{Ru}4d\varepsilon$ is relatively small in Sr_2RuO_4 , because of both the two-dimensionality and the symmetry of the atomic wave functions. We consider that the Hund's coupling is actually hard to be the main origin of the spin-triplet superconductivity in Sr_2RuO_4 .

Recently the present authors discussed on the basis of the one-band Hubbard model for the single branch γ .²⁸⁾ According to the previous works,^{28,29)} the spin-triplet superconductivity of Sr_2RuO_4 is a natural result of the electron correlations. Even if the spin susceptibility has no prominent peak around $\mathbf{q} = 0$, the effective pairing interaction has a momentum dependence favorable for the p -wave pairing state. The aim of the present article is to extend the previous single-band discussion to three-band one and give a comprehensive understanding on the mechanism of the p -wave pairing. As a result, we show the following points: the spin-triplet p -wave state is more stable than the spin-singlet d -wave state for moderately strong Coulomb interaction. One of the three bands, γ , plays the dominant role in the superconducting transition, and the pairing on the other two bands (α and β) is induced passively through the inter-orbit couplings. The most significant momentum dependence for the p -wave pairing originates from the vertex correction terms, and the incommensurate antiferromagnetic spin fluctuations are expected to disturb the p -wave pairing by enhancing the d -wave pairing. Therefore we can regard the spin-triplet superconductivity in Sr_2RuO_4 as one of the natural results of electron correlations, and cannot consider as a result of some strong magnetic fluctuations.

This paper is organized as follows. In § 2, we give the formulation including introduction of the

Hubbard Hamiltonian and perturbation expansion. In § 3, we show the results of the numerical calculations of T_c as a function of the Coulomb energy, anomalous self-energy and effective interaction. There we mention also normal Fermi liquid properties, Fermi surface, normal self-energy and density of states. Finally, in § 4, we comment on the results, give a proposal for experiments, and conclude the paper.

§2. Formulation

2.1 Three-band Hubbard model

Sr_2RuO_4 is one of typical strongly correlated electron systems where Ru4d electrons play the most significant role for the electronic properties. According to the band calculation results, Ru4d ε orbitals take the main part of the density of states near the Fermi level, although the Ru4d ε and O2p orbitals are hybridizing.^{12,13)} Therefore the electronic structure is expected to be reproduced well by considering three Wannier states, xy , yz and xz , which have the characters of Ru4d $_{xy,yz,xz}$.

We give the Hamiltonian in the form,

$$H = H_0 + H', \quad (1)$$

where H_0 and H' are the noninteracting part and interaction part, respectively. H_0 is given by

$$H_0 = \sum_{\mathbf{k}, \ell, \sigma} \xi_\ell(\mathbf{k}) c_{\mathbf{k}\ell\sigma}^\dagger c_{\mathbf{k}\ell\sigma} + \sum_{\mathbf{k}, \sigma} \lambda(\mathbf{k}) (c_{\mathbf{k}yz\sigma}^\dagger c_{\mathbf{k}xz\sigma} + c_{\mathbf{k}xz\sigma}^\dagger c_{\mathbf{k}yz\sigma}), \quad (2)$$

where $c^\dagger(c)$ is electron creation(annihilation) operator, and \mathbf{k} , $\sigma^{(i)}$ and ℓ denote momentum, spin and the Wannier states (xy, yz, xz), respectively. We take the following band dispersions,

$$\xi_{xy}(\mathbf{k}) = 2t_1(\cos k_x + \cos k_y) + 4t_2 \cos k_x \cos k_y - \mu_{xy}, \quad (3)$$

$$\xi_{yz}(\mathbf{k}) = 2t_3 \cos k_y + 2t_4 \cos k_x - \mu_{yz}, \quad (4)$$

$$\xi_{xz}(\mathbf{k}) = 2t_3 \cos k_x + 2t_4 \cos k_y - \mu_{xz}, \quad (5)$$

$$\lambda(\mathbf{k}) = 4\lambda_0 \sin k_x \sin k_y. \quad (6)$$

t_1, t_2, t_3, t_4 and λ_0 are transfer integrals between nearest or next nearest neighbor Ru sites (Fig. 1), where we have assumed tetragonal symmetry, and μ_ℓ is the chemical potential. For the present calculation, we take $t_1 = -1.00$, $t_2 = -0.400$, $t_3 = -1.25$, $t_4 = -0.125$ and $\lambda_0 = -0.200$, and determine the chemical potentials μ_ℓ to satisfy $n_{xy} = 0.700$, $n_{yz} = 0.700$ and $n_{xz} = 0.700$, where n_ℓ is the electron filling per one spin state in the orbital ℓ . The total population of the conduction electrons at a Ru site equals $2(n_{xy} + n_{yz} + n_{xz}) = 4.200$, which is a little larger than the electron number obtained by the experiments,¹¹⁾ 4.032. We discuss this deviation in § 4. We take the following on-site Coulomb interaction for the interacting part,

$$H' = \frac{1}{2}U \sum_i \sum_\ell \sum_{\sigma \neq \sigma'} c_{i\ell\sigma}^\dagger c_{i\ell\sigma'}^\dagger c_{i\ell\sigma'} c_{i\ell\sigma} + \frac{1}{2}U' \sum_i \sum_{\ell \neq \ell'} \sum_{\sigma, \sigma'} c_{i\ell\sigma}^\dagger c_{i\ell'\sigma'}^\dagger c_{i\ell'\sigma'} c_{i\ell\sigma}$$

$$+ \frac{1}{2}J \sum_i \sum_{\ell \neq \ell'} \sum_{\sigma, \sigma'} c_{i\ell\sigma}^\dagger c_{i\ell'\sigma'}^\dagger c_{i\ell\sigma'} c_{i\ell'\sigma} + \frac{1}{2}J' \sum_i \sum_{\ell \neq \ell'} \sum_{\sigma \neq \sigma'} c_{i\ell\sigma}^\dagger c_{i\ell'\sigma'}^\dagger c_{i\ell'\sigma'} c_{i\ell\sigma}. \quad (7)$$

J is the Hund's coupling. For the convenience of calculation, we express the Coulomb integrals by a matrix $I_{(\ell_1\sigma_1)(\ell_2\sigma_2),(\ell_3\sigma_3)(\ell_4\sigma_4)}$, where the matrix I has the following elements,

$$\left. \begin{aligned} I_{(\ell\sigma)(\ell\bar{\sigma}),(\ell\bar{\sigma})(\ell\sigma)} &= U \\ I_{(\ell\sigma)(\ell'\sigma),(\ell'\sigma)(\ell\sigma)} &= U' - J \\ I_{(\ell\sigma)(\ell'\bar{\sigma}),(\ell'\bar{\sigma})(\ell\sigma)} &= U' \\ I_{(\ell\sigma)(\ell'\bar{\sigma}),(\ell\bar{\sigma})(\ell'\sigma)} &= J \\ I_{(\ell\sigma)(\ell\bar{\sigma}),(\ell'\bar{\sigma})(\ell'\sigma)} &= J' \end{aligned} \right\}, \quad (8)$$

where $\ell \neq \ell'$, and $\sigma \neq \bar{\sigma}$, and the other elements are zero. Using the matrix I , H' is expressed in the simple form,

$$H' = \frac{1}{2} \sum_i \sum_{\zeta_1\zeta_2\zeta_3\zeta_4} I_{\zeta_1\zeta_2,\zeta_3\zeta_4} c_{i\zeta_1}^\dagger c_{i\zeta_2}^\dagger c_{i\zeta_3} c_{i\zeta_4}, \quad (9)$$

where we have adopted the short notations, $\zeta = (\ell\sigma)$ and $\sum_\zeta = \sum_\ell \sum_\sigma$. We define the antisymmetric bare vertex by

$$\Gamma_{\zeta_1\zeta_2,\zeta_3\zeta_4}^{(0)} = I_{\zeta_1\zeta_2,\zeta_3\zeta_4} - I_{\zeta_1\zeta_2,\zeta_4\zeta_3}. \quad (10)$$

In the perturbation expansion, this vertex is represented diagrammatically by the empty square as depicted in Fig. 2. If we have in mind the rotation invariance of the $d\epsilon$ atomic orbital wave functions in orbital space, the Coulomb integrals, U , U' , J and J' , are not independent parameters, and the relations $U = U' + 2J$ and $J = J'$ are derived.³⁰⁾ We cannot, however, easily tell that the relation should be valid even for the Wannier wave functions in metallic solids, because the Coulomb interaction may be changed effectively, in general, for example, due to the screening effect. In the present calculation, therefore we treat the Coulomb integrals as independent parameters. In any case, as we can see in §3.3, we obtain the p -wave superconductivity for a broad parameter region of the inter-orbit couplings, and may conclude that this assumption of the independence is not significant in the present discussions.

In the previous work, we investigated the magnetic properties of layered ruthenates on the basis of the same model.³¹⁾

2.2 Perturbation expansions

We expand the normal self-energy and the effective pairing interaction perturbatively up to the third order with respect to the Coulomb interaction H' . At first, we neglect the hybridizing term including $\lambda(\mathbf{k})$. In Sr_2RuO_4 , $\lambda(\mathbf{k})$ is the second nearest hopping term and expected to be small compared with the band width. By this simplification, the normal self-energy and the effective interaction are expanded perturbatively by the bare Green's functions,

$$G_\ell^{(0)}(k) = \frac{1}{i\omega_n - \xi_\ell(\mathbf{k})}, \quad (11)$$

where $\ell = \{xy, yz, xz\}$ and $k = (\mathbf{k}, i\omega_n)$.

In the present scheme, the normal self-energy has only the diagonal elements $\Sigma_\ell(k)$. The perturbation terms to be summed up are displayed in Fig. 3. Since the terms represented by Fig. 3(N1) only shift the chemical potentials μ_ℓ , we regard them as already included in μ_ℓ 's. The general forms of perturbation terms remained for summations are given as follows.

$$\Sigma_{\zeta_1\zeta_2}^{\text{N2}}(k) = -\frac{1}{2}\left(\frac{T}{N}\right)^2 \sum_{k_1, k_2} \sum_{\zeta_3\zeta_4} \sum_{\xi_1\xi_2\xi_3\xi_4} G_{\zeta_4\zeta_3}^{(0)}(k_1) G_{\xi_4\xi_2}^{(0)}(k_2) \times G_{\xi_3\xi_1}^{(0)}(k - k_1 + k_2) \Gamma_{\zeta_1\xi_2\xi_3\zeta_4}^{(0)} \Gamma_{\xi_1\zeta_3\zeta_2\xi_4}^{(0)}, \quad (12)$$

$$\begin{aligned} \Sigma_{\zeta_1\zeta_2}^{\text{N3a}}(k) = & -\left(\frac{T}{N}\right)^3 \sum_{k_1, k_2, k_3} \sum_{\zeta_3\zeta_4} \sum_{\xi_1\xi_2\xi_3\xi_4} \sum_{\gamma_1\gamma_2\gamma_3\gamma_4} G_{\zeta_4\zeta_3}^{(0)}(k_1) G_{\xi_4\xi_2}^{(0)}(k_2) G_{\xi_3\xi_1}^{(0)}(k - k_1 + k_2) \\ & \times G_{\gamma_4\gamma_2}^{(0)}(k_3) G_{\gamma_3\gamma_1}^{(0)}(k - k_1 + k_3) \Gamma_{\zeta_1\xi_2\xi_3\zeta_4}^{(0)} \Gamma_{\xi_1\gamma_2\gamma_3\xi_4}^{(0)} \Gamma_{\gamma_1\zeta_3\zeta_2\gamma_4}^{(0)}, \end{aligned} \quad (13)$$

$$\begin{aligned} \Sigma_{\zeta_1\zeta_2}^{\text{N3b}}(k) = & \frac{1}{4}\left(\frac{T}{N}\right)^3 \sum_{k_1, k_2, k_3} \sum_{\zeta_3\zeta_4} \sum_{\xi_1\xi_2\xi_3\xi_4} \sum_{\gamma_1\gamma_2\gamma_3\gamma_4} G_{\zeta_3\zeta_4}^{(0)}(k_1) G_{\xi_3\xi_2}^{(0)}(k_2) G_{\xi_4\xi_1}^{(0)}(k + k_1 - k_2) \\ & \times G_{\gamma_3\gamma_2}^{(0)}(k_3) G_{\gamma_4\gamma_1}^{(0)}(k + k_1 - k_3) \Gamma_{\zeta_1\zeta_4\xi_3\xi_4}^{(0)} \Gamma_{\xi_1\xi_2\gamma_3\gamma_4}^{(0)} \Gamma_{\gamma_1\gamma_2\zeta_3\zeta_2}^{(0)}. \end{aligned} \quad (14)$$

The factors $\frac{1}{2}$ and $\frac{1}{4}$ multiplied in the terms $\Sigma_{\zeta_1\zeta_2}^{\text{N2}}(k)$ and $\Sigma_{\zeta_1\zeta_2}^{\text{N3b}}(k)$ are necessary to avoid the redundancy in the summation. By the simplification mentioned above,

$$G_{\zeta\zeta'}^{(0)}(k) = G_\ell^{(0)}(k) \delta_{\zeta\zeta'}, \quad (15)$$

where $\zeta = (\ell\sigma)$, $\zeta' = (\ell'\sigma')$, and $\delta_{\zeta\zeta'} = \delta_{\ell\ell'}\delta_{\sigma\sigma'}$. The diagonal elements of the normal self-energy are reduced to

$$\begin{aligned} \Sigma_\ell(k) = & \frac{T}{N} \sum_{k_1} \sum_{\ell_2} G_{\ell_2}^{(0)}(k_1) \left[\frac{1}{2} \sum_{m_1 m_2} X_{m_1 m_2}^{(0)}(k - k_1) \sum_{\nu_1 \nu_2} \sum_{\sigma_2} \Gamma_{(\ell\sigma)(m_2\nu_2), (m_1\nu_1)(\ell_2\sigma_2)}^{(0)} \Gamma_{(m_1\nu_1)(\ell_2\sigma_2), (\ell\sigma)(m_2\nu_2)}^{(0)} \right. \\ & - \sum_{n_1 n_2} \sum_{m_1 m_2} X_{n_1 n_2}^{(0)}(k - k_1) X_{m_1 m_2}^{(0)}(k - k_1) \sum_{\tau_1 \tau_2} \sum_{\nu_1 \nu_2} \sum_{\sigma_2} \Gamma_{(\ell\sigma)(n_2\tau_2), (n_1\tau_1)(\ell_2\sigma_2)}^{(0)} \\ & \times \Gamma_{(n_1\tau_1)(m_2\nu_2), (m_1\nu_1)(n_2\tau_2)}^{(0)} \Gamma_{(m_1\nu_1)(\ell_2\sigma_2), (\ell\sigma)(m_2\nu_2)}^{(0)} \\ & - \frac{1}{4} \sum_{n_1 n_2} \sum_{m_1 m_2} \Phi_{n_1 n_2}^{(0)}(k + k_1) \Phi_{m_1 m_2}^{(0)}(k + k_1) \sum_{\tau_1 \tau_2} \sum_{\nu_1 \nu_2} \sum_{\sigma_2} \Gamma_{(\ell\sigma)(\ell_2\sigma_2), (n_1\tau_1)(n_2\tau_2)}^{(0)} \\ & \left. \times \Gamma_{(n_1\tau_1)(n_2\tau_2), (m_1\nu_1)(m_2\nu_2)}^{(0)} \Gamma_{(m_1\nu_1)(m_2\nu_2), (\ell\sigma)(\ell_2\sigma_2)}^{(0)} \right], \end{aligned} \quad (16)$$

where the functions, $X_{\ell\ell'}^{(0)}(q)$ and $\Phi_{\ell\ell'}^{(0)}(q)$, are calculated by

$$X_{\ell\ell'}^{(0)}(q) = -\frac{T}{N} \sum_k G_\ell^{(0)}(q + k) G_{\ell'}^{(0)}(k), \quad (17)$$

$$\Phi_{\ell\ell'}^{(0)}(q) = -\frac{T}{N} \sum_k G_\ell^{(0)}(q - k) G_{\ell'}^{(0)}(k). \quad (18)$$

The renormalized Green's functions are given by

$$G_\ell(k) = \frac{1}{i\omega_n - \Xi_\ell(k)}, \quad (19)$$

where $\Xi_\ell(k) = \xi_\ell(\mathbf{k}) + \Sigma_\ell(k) - \delta\mu_\ell$. $\delta\mu_\ell$ is determined to satisfy the relation

$$\delta n_\ell = \frac{T}{N} \sum_k (G_\ell(k) - G_\ell^{(0)}(k)) = 0. \quad (20)$$

Here we take into account the effect of the hybridizing term $\lambda(\mathbf{k})$. We consider the following renormalized Green's functions:

$$G_{xy,xy}(k) = \frac{1}{i\omega_n - \Xi_{xy}(k)}, \quad (21)$$

$$G_{yz,yz}(k) = \frac{1}{i\omega_n - \Xi_{yz}(k) - \frac{\lambda^2(\mathbf{k})}{i\omega_n - \Xi_{xz}(k)}}, \quad (22)$$

$$G_{xz,xz}(k) = \frac{1}{i\omega_n - \Xi_{xz}(k) - \frac{\lambda^2(\mathbf{k})}{i\omega_n - \Xi_{yz}(k)}}, \quad (23)$$

$$\begin{aligned} G_{yz,xz}(k) &= G_{xz,yz}(k) \\ &= \frac{\lambda(\mathbf{k})}{(i\omega_n - \Xi_{yz}(k))(i\omega_n - \Xi_{xz}(k)) - \lambda^2(\mathbf{k})}, \end{aligned} \quad (24)$$

and the other elements of $G_{\ell\ell'}(k)$ are zero. These Green's functions are the matrix elements of the operator $[i\omega_n - H_0 - (\Sigma - \delta\mu)]^{-1}$, where $\Sigma - \delta\mu$ is an operator with the diagonal matrix elements $(\Sigma_\ell(k) - \delta\mu_\ell)\delta_{\ell\ell'}$. Diagonalizing this renormalized Green's function, we obtain the following form

$$G_\nu(k) = \frac{1}{i\omega_n - \Xi_\nu(k)}. \quad (25)$$

Here $\nu = \{\alpha, \beta, \gamma\}$, and

$$\Xi_{\alpha,\beta}(k) = \Xi_\pm(k) \mp [\Xi_-^2(k) + \lambda^2(\mathbf{k})]^{\frac{1}{2}} \quad (26)$$

$$\Xi_\pm(k) = \frac{1}{2}(\Xi_{yz}(k) \pm \Xi_{xz}(k)) \quad (27)$$

$$\Xi_\gamma(k) = \Xi_{xy}(k) \quad (28)$$

Then we expand the anomalous self-energy perturbatively in a similar manner. The perturbation terms to be summed up are displayed diagrammatically in Fig. 4. The general forms for the perturbation terms are given as follows.

$$\Sigma_{\zeta_1\zeta_2}^{A1\dagger}(k) = -\frac{1}{2} \frac{T}{N} \sum_{k'} \sum_{\zeta_3\zeta_4} F_{\zeta_4\zeta_3}^\dagger(k') \Gamma_{\zeta_4\zeta_3,\zeta_2\zeta_1}^{(0)}, \quad (29)$$

$$\Sigma_{\zeta_1\zeta_2}^{A2\dagger}(k) = -\left(\frac{T}{N}\right)^2 \sum_{k',k_1} \sum_{\zeta_3\zeta_4} \sum_{\gamma_1\gamma_2\gamma_3\gamma_4} F_{\zeta_4\zeta_3}^\dagger(k') G_{\gamma_4\gamma_3}^{(0)}(k_1) G_{\gamma_2\gamma_1}^{(0)}(k + k_1 - k') \Gamma_{\zeta_4\gamma_3,\gamma_2\zeta_1}^{(0)} \Gamma_{\gamma_1\zeta_3,\zeta_2\gamma_4}^{(0)}, \quad (30)$$

$$\begin{aligned}\Sigma_{\zeta_1\zeta_2}^{\text{A3a}\dagger}(k) = & -\left(\frac{T}{N}\right)^3 \sum_{k',k_1,k_2} \sum_{\zeta_3\zeta_4} \sum_{\xi_1\xi_2\xi_3\xi_4} \sum_{\gamma_1\gamma_2\gamma_3\gamma_4} F_{\zeta_4\zeta_3}^\dagger(k') G_{\xi_4\xi_2}^{(0)}(k_1) G_{\xi_3\xi_1}^{(0)}(k-k'+k_1) \\ & \times G_{\gamma_4\gamma_2}^{(0)}(k_2) G_{\gamma_3\gamma_1}^{(0)}(k-k'+k_2) \Gamma_{\zeta_4\xi_2,\xi_3\zeta_1}^{(0)} \Gamma_{\xi_1\gamma_2,\gamma_3\xi_4}^{(0)} \Gamma_{\gamma_1\zeta_3,\zeta_2\gamma_4}^{(0)},\end{aligned}\quad (31)$$

$$\begin{aligned}\Sigma_{\zeta_1\zeta_2}^{\text{A3b}\dagger}(k) = & \left(\frac{T}{N}\right)^3 \sum_{k',k_1,k_2} \sum_{\zeta_3\zeta_4} \sum_{\xi_1\xi_2\xi_3\xi_4} \sum_{\gamma_1\gamma_2\gamma_3\gamma_4} F_{\zeta_4\zeta_3}^\dagger(k') G_{\gamma_1\gamma_2}^{(0)}(-k+k'+k_1) G_{\gamma_3\gamma_4}^{(0)}(k_1) \\ & \times G_{\xi_3\xi_2}^{(0)}(-k+k_1+k_2) G_{\xi_4\xi_1}^{(0)}(k_2) \Gamma_{\zeta_4\gamma_2,\gamma_3\zeta_1}^{(0)} \Gamma_{\gamma_4\xi_1,\zeta_2\xi_3}^{(0)} \Gamma_{\xi_2\zeta_3,\xi_4\gamma_1}^{(0)},\end{aligned}\quad (32)$$

$$\begin{aligned}\Sigma_{\zeta_1\zeta_2}^{\text{A3c}\dagger}(k) = & \left(\frac{T}{N}\right)^3 \sum_{k,k_1,k_2} \sum_{\zeta_3\zeta_4} \sum_{\xi_1\xi_2\xi_3\xi_4} \sum_{\gamma_1\gamma_2\gamma_3\gamma_4} F_{\zeta_4\zeta_3}^\dagger(k') G_{\gamma_3\gamma_4}^{(0)}(k-k'+k_1) G_{\gamma_1\gamma_2}^{(0)}(k_1) \\ & \times G_{\xi_3\xi_2}^{(0)}(k+k_1+k_2) G_{\xi_1\xi_4}^{(0)}(k_2) \Gamma_{\xi_4\gamma_2,\xi_3\zeta_1}^{(0)} \Gamma_{\gamma_4\zeta_3,\zeta_2\gamma_1}^{(0)} \Gamma_{\xi_2\zeta_4,\xi_1\gamma_3}^{(0)},\end{aligned}\quad (33)$$

$$\begin{aligned}\Sigma_{\zeta_1\zeta_2}^{\text{A3d}\dagger}(k) = & \frac{1}{2} \left(\frac{T}{N}\right)^3 \sum_{k,k_1,k_2} \sum_{\zeta_3\zeta_4} \sum_{\xi_1\xi_2\xi_3\xi_4} \sum_{\gamma_1\gamma_2\gamma_3\gamma_4} F_{\zeta_4\zeta_3}^\dagger(k') G_{\gamma_2\gamma_1}^{(0)}(k-k'+k_1) G_{\gamma_4\gamma_3}^{(0)}(k_1) \\ & \times G_{\xi_2\xi_3}^{(0)}(k+k_1-k_2) G_{\xi_4\xi_1}^{(0)}(k_2) \Gamma_{\zeta_4\gamma_3,\gamma_2\zeta_1}^{(0)} \Gamma_{\gamma_1\zeta_3,\xi_4\xi_2}^{(0)} \Gamma_{\xi_1\xi_3,\gamma_4\zeta_2}^{(0)},\end{aligned}\quad (34)$$

$$\begin{aligned}\Sigma_{\zeta_1\zeta_2}^{\text{A3e}\dagger}(k) = & \frac{1}{2} \left(\frac{T}{N}\right)^3 \sum_{k,k_1,k_2} \sum_{\zeta_3\zeta_4} \sum_{\xi_1\xi_2\xi_3\xi_4} \sum_{\gamma_1\gamma_2\gamma_3\gamma_4} F_{\zeta_4\zeta_3}^\dagger(k') G_{\gamma_4\gamma_3}^{(0)}(-k+k'+k_1) G_{\gamma_2\gamma_1}^{(0)}(k_1) \\ & \times G_{\xi_2\xi_4}^{(0)}(-k+k_1-k_2) G_{\xi_1\xi_3}^{(0)}(k_2) \Gamma_{\xi_3\xi_4,\gamma_2\zeta_1}^{(0)} \Gamma_{\zeta_4\gamma_3,\xi_2\xi_1}^{(0)} \Gamma_{\gamma_1\zeta_3,\zeta_2\gamma_4}^{(0)},\end{aligned}\quad (35)$$

where $F_{\zeta_4\zeta_3}^\dagger(k)$ is the anomalous Green's function. The factors $\frac{1}{2}$ multiplied in the (A1), (A3d) and (A3e) are necessary to avoid the redundancy in the summation. By summing up these contributions, we obtain the following Éliashberg equation within the third order perturbation theory.

$$\Sigma_{\zeta_1\zeta_2}^{\text{A}\dagger}(k) = -\frac{T}{N} \sum_{k'} \sum_{\zeta_3\zeta_4} F_{\zeta_4\zeta_3}^\dagger(k') \left(\Gamma_{\zeta_4\zeta_3,\zeta_2\zeta_1}(k',k) - \frac{1}{2} \Gamma_{\zeta_4\zeta_3,\zeta_2\zeta_1}^{(0)} \right), \quad (36)$$

where $\Gamma_{\zeta_4\zeta_3,\zeta_2\zeta_1}(k',k)$ is the renormalized pair scattering amplitude and given in the following,

$$\begin{aligned}\Gamma_{\zeta_4\zeta_3,\zeta_2\zeta_1}(k',k) = & \Gamma_{\zeta_4\zeta_3,\zeta_2\zeta_1}^{(0)} - \sum_{\gamma_1\gamma_3} X_{m_1m_3}^{(0)}(k-k') \Gamma_{\zeta_4\gamma_3,\gamma_1\zeta_1}^{(0)} \Gamma_{\gamma_1\zeta_3,\zeta_2\gamma_3}^{(0)} \\ & + \sum_{\gamma_1\gamma_2} \sum_{\xi_1\xi_2} X_{n_1n_2}^{(0)}(k-k') X_{m_1m_2}^{(0)}(k-k') \Gamma_{\zeta_4\xi_2,\xi_1\zeta_1}^{(0)} \Gamma_{\xi_1\gamma_2,\gamma_1\xi_2}^{(0)} \Gamma_{\gamma_1\zeta_3,\zeta_2\gamma_2}^{(0)} \\ & - \frac{T}{N} \sum_{k_1} \sum_{\gamma_1\gamma_3} \sum_{\xi_1\xi_2} G_{m_3}^{(0)}(-k+k'+k_1) \left[X_{n_2n_1}^{(0)}(-k+k_1) \Gamma_{\zeta_4\gamma_3,\gamma_1\zeta_1}^{(0)} \Gamma_{\gamma_1\xi_1,\zeta_2\xi_2}^{(0)} \Gamma_{\xi_2\zeta_3,\xi_1\gamma_3}^{(0)} \right.\end{aligned}$$

$$\begin{aligned}
& + \frac{1}{2} \Phi_{n_2 n_1}^{(0)}(-k + k_1) \Gamma_{\xi_2 \xi_1, \zeta_1 \gamma_1}^{(0)} \Gamma_{\zeta_4 \gamma_3, \xi_2 \xi_1}^{(0)} \Gamma_{\gamma_1 \zeta_3, \zeta_2 \gamma_3}^{(0)} \Big] G_{m_1}^{(0)}(k_1) \\
& - \frac{T}{N} \sum_{k_1} \sum_{\gamma_1 \gamma_3} \sum_{\xi_1 \xi_2} G_{m_3}^{(0)}(k - k' + k_1) \Big[X_{n_2 n_1}^{(0)}(k + k_1) \Gamma_{\xi_1 \gamma_1, \xi_2 \zeta_1}^{(0)} \Gamma_{\gamma_3 \zeta_3, \zeta_2 \gamma_1}^{(0)} \Gamma_{\xi_2 \zeta_4, \xi_1 \gamma_3}^{(0)} \\
& + \frac{1}{2} \Phi_{n_2 n_1}^{(0)}(k + k_1) \Gamma_{\zeta_4 \gamma_1, \gamma_3 \zeta_1}^{(0)} \Gamma_{\gamma_3 \zeta_3, \xi_1 \xi_2}^{(0)} \Gamma_{\xi_1 \xi_2, \gamma_1 \zeta_2}^{(0)} \Big] G_{m_1}^{(0)}(k_1). \tag{37}
\end{aligned}$$

Here we have adopted the short notations, $\zeta_i = (\ell_i \sigma_i)$, $\gamma_i = (m_i \nu_i)$ and $\xi_i = (n_i \tau_i)$. We assume the pairing interaction binds the most strongly the quasi-particles on the same band, and consider the three components of the anomalous Green's function and the anomalous self-energy, $F_{\nu\sigma\sigma'}^\dagger(k)$ and $\Sigma_{\nu\sigma\sigma'}^{\text{A}\dagger}(k)$, where $\nu = \alpha, \beta, \gamma$. The diagonalized band indices $\nu (= \alpha, \beta, \gamma)$ are replaced by the orbital indices $\ell (= xy, yz, xz)$ through the following relations,

$$F_{\zeta\zeta'}^\dagger(k) = \sum_{\nu=\alpha,\beta,\gamma} U_{\ell\nu}^{(0)}(\mathbf{k}) U_{\ell'\nu}^{(0)}(\mathbf{k}) F_{\nu\sigma\sigma'}^\dagger(k) \tag{38}$$

$$\begin{aligned}
& = \sum_{\nu=\alpha,\beta,\gamma} U_{\ell\nu}^{(0)}(\mathbf{k}) U_{\ell'\nu}^{(0)}(\mathbf{k}) |G_\nu(k)|^2 \Sigma_{\nu\sigma\sigma'}^{\text{A}\dagger}(k) \\
\Sigma_{\nu\sigma\sigma'}^{\text{A}\dagger}(k) & = \sum_{\ell\ell'} U_{\nu\ell}^{(0)-1}(\mathbf{k}) U_{\nu\ell'}^{(0)-1}(\mathbf{k}) \Sigma_{\zeta\zeta'}^{\text{A}\dagger}(k), \tag{39}
\end{aligned}$$

where $\zeta = (\ell\sigma)$, $\zeta' = (\ell'\sigma')$, and $\hat{U}^{(0)}(\mathbf{k})$ is a matrix for the diagonalization of the noninteracting Hamiltonian H_0 ,

$$\hat{U}^{(0)}(\mathbf{k}) = \begin{array}{c} \gamma \quad \alpha \quad \beta \\ \begin{array}{ccc} xy & \begin{bmatrix} 1 & 0 & 0 \end{bmatrix} \\ yz & \begin{bmatrix} 0 & K(\mathbf{k}) & L(\mathbf{k}) \end{bmatrix} \\ xz & \begin{bmatrix} 0 & -L(\mathbf{k}) & K(\mathbf{k}) \end{bmatrix} \end{array} \end{array}, \tag{40}$$

where

$$K(\mathbf{k}) = \sqrt{\frac{1}{2}(1 - M(\mathbf{k}))}, \tag{41}$$

$$L(\mathbf{k}) = \text{sgn}(\lambda(\mathbf{k})) \sqrt{\frac{1}{2}(1 + M(\mathbf{k}))}, \tag{42}$$

$$M(\mathbf{k}) = \frac{\xi_-(\mathbf{k})}{\sqrt{\xi_-^2(\mathbf{k}) + \lambda^2(\mathbf{k})}}, \tag{43}$$

$$\xi_-(\mathbf{k}) = \frac{1}{2}(\xi_{yz}(\mathbf{k}) - \xi_{xz}(\mathbf{k})). \tag{44}$$

We replace the left hand side of the eq. (36) by $\lambda(T) \Sigma_{\zeta_1 \zeta_2}^{\text{A}\dagger}(q)$, and determine the transition temperature, at which the eigenvalue $\lambda(T)$ equals unity ($\lambda(T_c) = 1.00$), by solving the set of the equations eqs. (36)-(39). It is convenient to express the anomalous self-energy in the following form.²⁹⁾ For triplet pair,

$$\Sigma_{\nu\sigma\sigma'}^{\text{A}}(k) = [\mathbf{i}(\mathbf{D}_\nu(k) \cdot \boldsymbol{\sigma}) \sigma_y]_{\sigma\sigma'}, \tag{45}$$

and for singlet pair,

$$\Sigma_{\nu\sigma\sigma'}^A(k) = [i\Psi_\nu(k)\sigma_y]_{\sigma\sigma'}, \quad (46)$$

where σ is the Pauli matrix, and the function, $\mathbf{D}_\nu(k)$ ($\Psi_\nu(k)$), behaves as a vector(scalar) under the rotation in the spin space. In the numerical calculation, we assume the vector $\mathbf{D}_\nu(k)$ is perpendicular to the basal plane,

$$\mathbf{D}_\nu(k) = D_\nu(k)\hat{z}. \quad (47)$$

The direction is consistent with the experimental results of Knight shift.³⁾ This assumption is not substantial in the present calculation, because we do not introduce any anisotropy in the spin space. We can show that, if we take other direction of the vector, we obtain the same transition temperature. In order to determine the direction of the vector $\mathbf{D}_\nu(k)$, we must take into account the effect of the spin-orbit coupling.²⁶⁾ We do not consider that the spin-orbit coupling is essential for discussing a mechanism of the spin-triplet superconductivity in Sr_2RuO_4 .

Here we define the function, $\Gamma_{\nu'\sigma_4\sigma_3,\nu\sigma_2\sigma_1}(k',k)$, by

$$\Gamma_{\nu'\sigma_4\sigma_3,\nu\sigma_2\sigma_1}(k',k) = \sum_{\ell_1\ell_2\ell_3\ell_4} U_{\ell_4\nu'}^{(0)}(\mathbf{k}')U_{\ell_3\nu'}^{(0)}(\mathbf{k}')\Gamma_{\zeta_4\zeta_3,\zeta_2\zeta_1}(k',k)U_{\nu\ell_2}^{(0)-1}(\mathbf{k})U_{\nu\ell_1}^{(0)-1}(\mathbf{k}). \quad (48)$$

As we see in § 3.6, the component for the parallel spin pair on the γ band, $\Gamma_{\gamma\sigma\sigma,\gamma\sigma\sigma}(k',k)$, possesses a momentum dependence favoring p -wave pairing.

In conclusion of this section, note that the normal self-energy and the effective interaction have been expanded up to the third order in Coulomb energy by using only the bare $G_\ell^{(0)}(k)$ ($\ell = \{xy, yz, xz\}$), but the quasi-particles forming Cooper pair are described by the renormalized $G_\nu(k)$ $\nu = \{\alpha, \beta, \gamma\}$.

§3. Results of Calculation

3.1 Details of numerical calculations

The momentum and frequency summations appearing in the equations, (16)-(18), (36) and (37) can be performed numerically with use of fast Fourier transformation algorithm. For the numerical calculations, the first Brillouin zone is divided into 128×128 \mathbf{k} -meshes, and the number of Matsubara frequencies taken is $N_f = 1024$. The temperature region for numerical calculations is bounded from below by $T > W/2\pi N_f \approx 0.0012$, where W is the noninteracting band width. All of the numerical calculations in the present paper are performed in $T \geq 0.00250$. This lower bound corresponds to about 10(K), if we assume the band width W is about 2(eV), and is still higher than the real T_c of Sr_2RuO_4 , 1.5(K). Therefore we must extrapolate the calculation results of T_c to the weak interaction region.

3.2 Normal Fermi liquid state properties

We show here the results of the quantities related to the normal Fermi liquid state.

The Fermi surface consists of three sheets as depicted in Fig. 5. The circle around the point (π, π) , α , is hole-like, while the large circles around the corners, β and γ , enclose electrons. These results are in good agreement with those obtained by de Haas-van Alphen measurements¹¹⁾ and recent angle-resolved-photoemission measurements.³²⁾

The normal self-energy on the γ band as a function of frequency, $\Sigma_\gamma(\mathbf{k}_F, \omega)$, is shown in Fig. 6. We can see usual Fermi liquid behaviors for every case of various inter-orbit couplings, $\text{Re}\Sigma(\omega) \sim c\omega$ and $\text{Im}\Sigma(\omega) \sim c'\omega^2$ ($c, c' < 0$) at low energy ($\omega \sim 0$). The remarkable property which we would like to point out here is that inter-orbit couplings do not affect the normal self-energy in the low energy region $\omega \approx 0$, while they do in the high energy region. This is partly due to the situation where the hybridization among the localized orbits, xy , yz and xz , is not so large in Sr_2RuO_4 . As far as we discuss low energy phenomena, such as superconductivity, therefore, we may expect that the single-band approach²⁸⁾ is a good starting point.

Next we show the density of states(DOS) for a typical case in Fig. 7. The DOS of each band ν ($= \alpha, \beta, \gamma$) is calculated by the formula,

$$\rho_\nu(\omega) = -\frac{1}{\pi} \sum_{\mathbf{k}} \text{Im} G_\nu^R(\mathbf{k}, \omega), \quad (49)$$

where $G_\nu^R(k)$ is obtained by continuing analytically $G_\nu(k)$ from the upper half plane. What we should note is the large DOS peak near the Fermi level. This peak originates from the van Hove singularity on the two-dimensional band γ . As pointed out by Singh,¹³⁾ if the Fermi level comes above the singularity, the Fermi surface γ changes its topology, from electron-like circle to hole-like circle around the point (π, π) . The γ band takes the main part of the DOS at the Fermi level. This agrees with the results of the de Haas-van Alphen measurements.¹¹⁾ As a result, the γ band is expected to be significant in discussing the electronic properties of Sr_2RuO_4 .

3.3 Eigenvalues for triplet p -wave and singlet d -wave states

We show the calculation results of the maximum eigenvalues for the spin-triplet and the singlet states in Fig. 8. There we show the calculation results for four cases of relatively strong inter-orbit couplings. The orbital symmetry of the state giving the maximum eigenvalues is p -wave for the spin-triplet state and $d_{x^2-y^2}$ -wave for the spin-singlet state. In the cases (a), (b) and (d), we obtain the larger eigenvalues for the spin-triplet state than for the spin-singlet state at low temperatures. Therefore we expect that the p -wave state is realized for the three cases. For the case (c), where the Hund's coupling is strong, we can see that the eigenvalues for the p -wave state is small compared with those for the $d_{x^2-y^2}$ state. The reason why the $d_{x^2-y^2}$ -wave pairing state becomes more stable than p -wave one, as the strength of the inter-orbit coupling increases, will be discussed in § 4. It should be noted here that the values of inter-orbit couplings in the cases, (a), (b) and (c) are too large. We consider that actually they should be smaller, since in general they are weakened more by the screening effects than the intra-orbit coupling U . If we take smaller realistic inter-orbit

couplings, for example, as in the case (d), $d_{x^2-y^2}$ -wave state is not expected to be realized at all. Note that the situations for which we have given the results of eigenvalues here are still relatively unfavorable for the p -wave state because of the strong inter-orbit couplings.

3.4 Transition temperature for triplet p -wave state

The calculated transition temperature for the p -wave state is displayed in Fig. 9 as a function of U . In the both cases of the inter-orbit couplings, (a) and (b), we may obtain higher transition temperature for the p -wave state, according to the results of calculation of eigenvalues in § 3.3. We consider that the lower bound of temperature for the calculation, $T = 0.00300$, corresponds to about 10(K). We may obtain the more realistic value of $T_c=1.5$ (K), by extrapolating the results down to the smaller U region. According to the results, T_c becomes high for strong inter-orbit couplings. In the limit of weak inter-orbit coupling, we obtain the same results as we did in the previous single-band analysis for the γ band.

3.5 Momentum dependence of anomalous self-energy parts

The momentum dependence of the anomalous self-energy $D_\nu(k)$ is plotted in the Fig. 10, where we consider the state with the k_y -like symmetry $D_\nu(k_x, k_y, i\omega_n) = -D_\nu(k_x, -k_y, i\omega_n)$. The results show highly anisotropic p -wave state, and not f -wave. If we assume in the beginning the condition, $D_\nu(k_x, k_y, i\omega_n) = -D_\nu(-k_x, k_y, i\omega_n)$, we obtain the p -wave state with the k_x -like symmetry. The relative phases of $D_\nu(k)$'s converge to zero, and we can assume without any loss of the generality that $D_\nu(k)$'s are real.

We should note that the magnitude of the anomalous self-energy is the largest on the γ Fermi surface. This is “orbital dependent superconductivity”, which was proposed originally by Agterberg *et al.*³³⁾ The magnitudes of $D_\alpha(k)$ and $D_\beta(k)$ are almost the same, since both of the α and the β bands are constructed by hybridizing the original one-dimensional yz and xz bands. The γ band originates mainly from the two-dimensional xy band, and is separated from the other two bands, α and β , in that the hybridization is expected to be small (In the present theoretical formulation, the hybridization is assumed to be exactly zero, since we consider only the single RuO_2 layer). In Fig. 10, we have shown the case of relatively strong inter-orbit couplings. If we take small inter-orbit couplings, the relative magnitude of $D_\gamma(k)$ to $D_{\alpha,\beta}(k)$ becomes large. In the unrealistic and extreme case where inter-orbit couplings are zero ($U' = J = J' = 0$), $D_\alpha(k)$ and $D_\beta(k)$ converge to zero, and only $D_\gamma(k)$ converges to a finite value. As a consequence, we find that the γ band dominates the superconducting transition. Here we have shown only the results for the triplet p -wave state. According to our calculation, the dominance of the γ band is also valid for the case of the singlet $d_{x^2-y^2}$ -wave state.

3.6 Momentum dependence of effective pairing interaction on the γ band

We extract only the pair scattering amplitude of quasi-particles from the γ band to the γ band. This channel is the most significant not only for the p -wave pairing but also for the $d_{x^2-y^2}$ -wave pairing. In Fig. 11 we show the plots of the vertex functions (a) $\Gamma_{\gamma\sigma\sigma,\gamma\sigma\sigma}(k',k)$ for the parallel spin pairs and (b) $\Gamma_{\gamma\sigma\bar{\sigma},\gamma\bar{\sigma}\sigma}(k',k)$ for the anti-parallel spin pairs.

In the triplet case (Fig. 11(a)), we find that the function $\Gamma_{\gamma\sigma\sigma,\gamma\sigma\sigma}(k',k)$, has a maximum value around the point $\mathbf{k} \approx -\mathbf{k}'$. This feature originates from the vertex correction terms (mainly, (A3d) and (A3e) in Fig. 4), and not from the exchange of any bosonic excitations. This characteristic momentum dependence of the vertex function is the origin of the relatively high transition temperature for the triplet pairing state, and is basically the same one as derived in the previous work for the single-band Hubbard model.²⁸⁾

In the singlet case (Fig. 11(b)), $\Gamma_{\gamma\sigma\bar{\sigma},\gamma\bar{\sigma}\sigma}(q;k)$ shows the characteristic peak around $\mathbf{k} = \mathbf{k}' + \mathbf{Q}_{\text{IAF}}$, where $\mathbf{Q}_{\text{IAF}} \approx (\pm 0.6\pi, \pm 0.6\pi)$. These peaks are due to the nesting of the quasi-one-dimensional Fermi surfaces, yz and xz (or almost equivalently, α and β). This momentum dependence was observed as sizeable incommensurate antiferromagnetic spin fluctuations by the inelastic neutron scattering measurements,¹⁷⁾ and was obtained also by the theoretical calculations on the magnetic properties of Sr_2RuO_4 .^{34,31)} Since it is through the inter-orbit couplings that the momentum dependence of the incommensurate fluctuations is reflected in the pairing interaction on the γ band, the peaks around $\mathbf{k} = \mathbf{k}' + \mathbf{Q}_{\text{IAF}}$ vanish as the strength of the inter-orbit couplings is decreased. On the other hand, the large values of the vertex function around $\mathbf{k} \approx \mathbf{k}'$ are due to the ferromagnetic components of the susceptibility for the $xy(\gamma)$ band. Note that the values of the vertex function $\Gamma_{\gamma\sigma\bar{\sigma},\gamma\bar{\sigma}\sigma}(k',k)$ are positive all over the Brillouin zone. This is because of the on-site repulsion U . In general this is the reason why conventional s -wave superconductivity is not expected to be realized in strongly correlated electron systems.

Note that, as mentioned in § 3.3, the cases we have shown here are the strong inter-orbit coupling ones. We consider that the inter-orbit couplings are actually not so strong. We have assumed such strong inter-orbit couplings to elucidate their roles.

§4. Discussion and Conclusion

In this section, we would like to discuss the results of calculation comprehensively, and give some proposals on experiments, based on our microscopic picture of the superconductivity in Sr_2RuO_4 .

In § 2.1, we have taken the electron filling per one spin state, $n_{xy} = n_{yz} = n_{xz} = 0.700$. This seems to be a little large compared with the results of the de Haas-van Alphen measurements,¹¹⁾ although the Fermi surfaces for this filling reproduce the observed ones qualitatively well, as shown in § 3.2. According to the measurements, it is plausible that the orbits are filled as the total electron number equals 4.032. If we assume that all of the three orbits are filled with even number of electrons, the electron number of one orbit is $n_\ell = 0.672$. If we take the filling $n_\ell = 0.672$ in the

calculation, the parameter region of the inter-orbit couplings where the p -wave state overcomes the $d_{x^2-y^2}$ -wave state is limited only in the weak inter-orbit couplings. We consider, however, that this situation is unrealistic, because $d_{x^2-y^2}$ -wave state has never been observed experimentally near the triplet superconducting phase of Sr_2RuO_4 . We relax the relation $2(n_{xy} + n_{yz} + n_{xz}) = 4.032$ in order to obtain the good agreement with the realistic situation. The incommensurate nesting vector $\mathbf{Q}_{\text{IAF}} (= (Q_{\text{IAF}x}, Q_{\text{IAF}y}, 0))$ is estimated by $Q_{\text{IAF}y} \approx 2(1 - n_{yz})\pi$ and $Q_{\text{IAF}x} \approx 2(1 - n_{xz})\pi$. The observed nesting vector is $Q_{\text{IAF}x} = Q_{\text{IAF}y} = 0.60\pi$.¹⁷⁾ Therefore we should take $n_{yz} = n_{xz} = 0.700$, and we have assumed that the three orbits are almost degenerate and $n_{xy} = 0.700$. At the present stage, the theory proposed here suggests that Sr_2RuO_4 seems to be located near the boundary of the p -wave and the $d_{x^2-y^2}$ states in the parameter space. We consider, however, that the present theory may be still insufficient for discussing quantitatively the competition of the p -wave and the $d_{x^2-y^2}$ -wave pairing states. In the future, it must be proved by more refined theoretical treatments that the $d_{x^2-y^2}$ -wave pairing state is more suppressed. One way of the further study is to inspect the effect of the higher order terms. In any case, we believe that, as far as we discuss only the mechanism of the p -wave superconductivity in Sr_2RuO_4 , the theory gives a satisfactory result, in that we have obtained the relatively high T_c for the p -wave state and the momentum dependence which favors the pairing state, as shown in Figs. 9 and 11(a).

In § 3.3 we have shown that for the strong inter-orbit couplings, particularly for the strong Hund's coupling, the eigenvalues for the $d_{x^2-y^2}$ -wave state become large compared with those for the p -wave state. This is because the stronger the inter-orbit coupling becomes, the more prominently the incommensurate spin fluctuations are reflected in the pairing interaction on the γ band. As the present authors pointed out in the previous work on the magnetic properties of quasi-two-dimensional ruthenates,³¹⁾ the Hund's coupling enhances the incommensurate fluctuations rather than the ferromagnetic components of the spin susceptibility. Therefore we may conclude that the Hund's coupling disturbs the p -wave pairing by enhancing the d -wave pairing.

As shown in § 3.5, the orbital symmetry of the pairing is anisotropic p -wave. In general, if we assume the most promising form of the vector $\mathbf{d}(\mathbf{k}) \sim (k_x \pm ik_y)\hat{z}$,³⁵⁾ we usually expect the nodeless gap around the cylindrical Fermi surface. The nodeless energy gap in Sr_2RuO_4 has, however, been considered to be inconsistent with the observed power-law behaviors in various quantities at low temperatures.^{6,9,36,37)} Recently we have successfully shown that the p -wave superconducting gap derived in the present formulation is quite consistent with the power-law behavior of the specific heat below T_c .³⁸⁾ There the strong momentum dependence of the anomalous self-energy is essential for a node-like structure on the β Fermi surface, and results in the power-law behavior at the low temperature. Accordingly, we would like to point out here that the p -wave state obtained in our discussions can explain the power-law behaviors of the specific heat, even if we assume the symmetry $\mathbf{d}(\mathbf{k}) \sim (k_x \pm ik_y)\hat{z}$.

We would like to give some proposals for experiments, based on our microscopic picture on the superconductivity of Sr_2RuO_4 . Let us consider that the number of electrons in the band $\gamma(xy)$ is increased. In such a case, as we previously showed in the single-band analysis for the γ band,²⁸⁾ the superconducting transition temperature is expected to be enhanced. This is due to the situation where, if we increase the electrons in γ band, the Fermi level becomes close to the van Hove singularity on the γ band and the density of states at the Fermi level is increased. Note here that the van Hove singularity is located only slightly above the Fermi level, as shown in Fig. 7. At the same time, as we insisted in the previous work,³¹⁾ the ferromagnetic components of the spin susceptibility may be enhanced. Carrier dopings by chemical substitution usually not only change the carrier number but also damage the conducting RuO_2 plane. Since the triplet superconductivity is sensitively destroyed by disorders, we should not take any chemical substitution for the carrier doping. We think that the most practical way of increasing the electron number in the γ band without damaging the RuO_2 layers at all is application of the uniaxial pressure along the c -axis. The orbits yz and xz spatially extends along the c -axis, while the orbit xy will be flat along the basal plane. If we apply the uniaxial pressure, the energy levels of the orbits yz and xz are lifted due to the crystalline field effect, while the xy orbit is not. Therefore we may expect that the electrons are transferred from the yz and the xz orbits to the xy orbit. Consequently, we would like to point out the following possibility. If we can indeed transfer the electrons from the yz and the xz orbits to the xy orbit by applying the uniaxial pressure, the transition temperature may become higher. At the same time, the system may become close to the ferromagnetism, as we suggested in the previous work.³¹⁾ Measuring the transition temperature and the uniform spin susceptibility under the uniaxial pressure along the c -axis is, therefore, very interesting. Recent experimental work on the elastic moduli suggests the possibility that the transition temperature is increased by applying the uniaxial pressure along the c -axis.³⁹⁾ We may consider the fact as an evidence that the superconducting transition occurs predominantly on the γ band. This experimental fact supports the p -wave pairing rather than the d -wave pairing, because, if the $d_{x^2-y^2}$ -wave state was realized, the transition temperature should become lower by increasing the electron number of the γ band, according to our previous work.²⁸⁾

In conclusion, we summarize the main results obtained. We have discussed a mechanism of the spin-triplet superconductivity in Sr_2RuO_4 . We can obtain the p -wave pairing state for moderately strong inter-orbit couplings. There one of the three bands, γ , plays the dominant role in the superconducting transition, and the pairing on the other two bands(α and β) is induced passively through the inter-orbit couplings. The most significant momentum dependence for the p -wave pairing originates from the vertex correction terms, and is basically the same one as we obtained in the previous single-band analysis.²⁸⁾ Therefore we should regard the spin-triplet superconductivity in Sr_2RuO_4 as one of the natural results of electron correlations, and cannot consider as a result

of some strong magnetic fluctuations. We would like to insist that Sr_2RuO_4 realizes the p -wave superconductivity which is basically described by a simple one-band repulsive Hubbard model.²⁸⁾

Acknowledgments

The authors are grateful for the useful discussions to Professor Y. Maeno, Professor M. Sigrist, Professor K. Ishida and Dr. N. Kikugawa. They would like to thank Dr. N. Okuda and Professor T. Suzuki for the generosity. Numerical calculations in this work were performed at the Yukawa Institute Computer Facility.

-
- [1] Y. Maeno, H. Hashimoto, K. Yoshida, S. Nishizaki, T. Fujita, J. G. Bednorz, and F. Lichtenberg: *Nature* **372** (1994) 532.
 - [2] Y. Maeno, T. M. Rice and M. Sigrist: *Phys. Today* **54** (2001) 42.
 - [3] K. Ishida, H. Mukuda, Y. Kitaoka, K. Asayama, Z. Q. Mao, Y. Mori and Y. Maeno: *Nature* **396** (1998) 658.
 - [4] J. A. Duffy, S. M. Hayden, Y. Maeno, Z. Q. Mao, J. Kulda and G. J. McIntyre: *Phys. Rev. Lett.* **85** (2000) 5412.
 - [5] A. P. Mackenzie, R. K. W. Haselwimmer, A. W. Tyler, G. G. Lonzarich, Y. Mori, S. Nishizaki and Y. Maeno: *Phys. Rev. Lett.* **80** (1998) 161.
 - [6] K. Ishida, H. Mukuda, Y. Kitaoka, Z. Q. Mao, Y. Mori and Y. Maeno: *Phys. Rev. Lett.* **84** (2000) 5387.
 - [7] G. M. Luke, Y. Fudamoto, K. M. Kojima, M. I. Larkin, J. Merrin, B. Nachumi, Y. J. Uemura, Y. Maeno, Z. Q. Mao, Y. Mori, H. Nakamura and M. Sigrist: *Nature* **394** (1998) 558.
 - [8] Z. Q. Mao, Y. Maeno, S. Nishizaki, T. Akima and T. Ishiguro: *Phys. Rev. Lett.* **84** (2000) 991.
 - [9] S. Nishizaki, Y. Maeno and Z. Q. Mao: *J. Phys. Soc. Jpn.* **69** (2000) 572.
 - [10] Y. Maeno, K. Yoshida, H. Hashimoto, S. Nishizaki, S. Ikeda, M. Nohara, T. Fujita, A. P. Mackenzie, N. E. Hussey, J. G. Bednorz and F. Lichtenberg: *J. Phys. Soc. Jpn.* **66** (1997) 1405.
 - [11] A. P. Mackenzie, S. R. Julian, A. J. Diver, G. J. McMullan, M. P. Ray, G. G. Lonzarich, Y. Maeno, S. Nishizaki and T. Fujita: *Phys. Rev. Lett.* **76** (1996) 3786.
 - [12] T. Oguchi: *Phys. Rev. B* **51** (1995) 1385.
 - [13] D. J. Singh: *Phys. Rev. B* **52** (1995) 1358.
 - [14] T. M. Rice and M. Sigrist: *J. Phys. Condens. Matter* **7** (1995) L643.
 - [15] I. I. Mazin and D. J. Singh: *Phys. Rev. Lett.* **79** (1997) 733.
 - [16] P. Monthoux and G. G. Lonzarich: *Phys. Rev. B* **59** (1999) 14598.
 - [17] Y. Sidis, M. Braden, P. Bourges, B. Hennion, S. Nishizaki, Y. Maeno and Y. Mori: *Phys. Rev. Lett.* **83** (1999) 3320.
 - [18] T. Kuwabara and M. Ogata: *Phys. Rev. Lett.* **85** (2000) 4586.
 - [19] K. Kuroki, M. Ogata, R. Arita and H. Aoki: *Phys. Rev. B* **63** (2001) 060506.
 - [20] F. Servant, B. Fak, S. Raymond, J. P. Brison, P. Lejay and J. Flouquet: *Phys. Rev. B* **65** (2002) 184511.
 - [21] M. Minakata and Y. Maeno: *Phys. Rev. B* **63** (2001) 180504(R).
 - [22] M. Braden, O. Friedt, Y. Sidis, P. Bourges, M. Minakata and Y. Maeno: *cond-mat/0107579*.
 - [23] N. Kikugawa and Y. Maeno: Preprint.
 - [24] T. Takimoto: *Phys. Rev. B* **62** (2000) R14641.
 - [25] G. Baskaran: *Physica B*: **223 & 224** (1996) 490.
 - [26] K. K. Ng and M. Sigrist: *Euro. Phys. Lett.* **49** (2000) 473.

- [27] J. Spalek: Phys. Rev. B **63** (2001) 104513.
- [28] T. Nomura and K. Yamada: J. Phys. Soc. Jpn. **69** (2000) 3678.
- [29] T. Nomura and K. Yamada: J. Phys. Chem. Solids **63** (2002) 1337.
- [30] For example, E. Dagotto, T. Hotta and A. Moreo: Phys. Rep. **344** (2001) 1.
- [31] T. Nomura and K. Yamada: J. Phys. Soc. Jpn. **69** (2000) 1856.
- [32] A. Damascelli, K. M. Shen, D. H. Lu, N. P. Armitage, F. Ronning, D. L. Feng, C. Kim, Z.-X. Shen, T. Kimura, Y. Tokura, Z. Q. Mao and Y. Maeno: J. Electron Spectr. Relat. Phenom. **114** (2001) 641.
- [33] D. F. Agterberg, T. M. Rice and M. Sigrist: Phys. Rev. Lett. **78** (1997) 3374.
- [34] I. I. Mazin and D. J. Singh: Phys. Rev. Lett. **82** (1999) 4324.
- [35] M. Sigrist, D. Agterberg, A. Furusaki, C. Honerkamp, K. K. Ng, T. M. Rice and M. E. Zhitomirsky: Physica C **317-318** (1999) 134.
- [36] I. Bonalde, B. D. Yanoff, M. B. Salamon, D. J. Van Harlingen and E. M. E. Chia: Phys. Rev. Lett. **85** (2000) 4775.
- [37] C. Lupien, W. A. MacFarlane, C. Proust, L. Taillefer, Z. Q. Mao and Y. Maeno: Phys. Rev. Lett. **86** (2001) 5986.
- [38] T. Nomura and K. Yamada: J. Phys. Soc. Jpn. **71** (2002) 404.
- [39] N. Okuda, T. Suzuki, Z. Q. Mao, Y. Maeno and T. Fujita: J. Phys. Soc. Jpn. **71** (2002) 1134; Physica B, **312-313** (2002) 800.

Fig. 1. Schematic illustration of single RuO₂ layer. The Ru4d_{xy,yz,xz} and O2p_{x,y,z} orbitals construct the two-dimensional network by hybridizing with each other.

Fig. 2. The antisymmetric bare vertex, $\Gamma_{\zeta_1\zeta_2,\zeta_3\zeta_4}^{(0)}$.

Fig. 3. Perturbation terms for normal self-energy up to the third order. The shaded circle in (N1) represents arbitrary self-energy insertion. The solid line and the empty square denote the bare Green's function $G_\ell^{(0)}(k)$ and the bare antisymmetric vertex $\Gamma^{(0)}$, respectively.

Fig. 4. Perturbation terms for anomalous self-energy up to the third order. The thin solid line, the thick solid line and the empty square denote the bare Green's function $G_\ell^{(0)}(k)$, the anomalous Green's function $F_{\zeta\zeta'}^\dagger(k)$ and the antisymmetric bare vertex $\Gamma^{(0)}$, respectively.

Fig. 5. The Fermi surface. The Coulomb integrals are $U = 3.731$, $U' = 0.300U$, $J = J' = U'$, and the temperature is $T = 0.0100$.

Fig. 6. The normal self-energy on the γ Fermi surface as a function of frequency. (a) real part, (b) imaginary part.

Fig. 7. The density of states. The Fermi level corresponds to $\omega = 0$. (a) The total density of states. (b) The partial density of states for the three bands, α , β and γ . The inset shows the details near the Fermi level.

Fig. 8. The maximum eigenvalues as a function of temperature T . For all of the cases, the intra-orbit coupling is fixed as $U = 3.079$. (a) $U' = 0.500U$, $J = J' = 0.667U'$. (b) $U' = 0.500U$, $J = J' = U'$. (c) $U' = 0.500U$, $J = J' = 1.333U'$. (d) $U' = 0.300U$, $J = J' = U'$. In the cases, (a), (b) and (d), we expect that the spin-triplet p -wave state is stable compared with the spin-singlet $d_{x^2-y^2}$ state.

Fig. 9. Transition temperature as a function of U for spin-triplet p -wave state. (a) $J = J' = 0.667U'$. (b) $J = J' = U'$.

Fig. 10. Contourplots of the results of $D_\nu(\mathbf{k}, i\pi T)$ ($\nu = \alpha, \beta, \gamma$). In the light and the dark colored regions, the functions take higher and lower values, respectively. The thick line circles represent the Fermi surfaces. The parameters are $U = 3.385$, $U' = 0.500U$, $J = J' = U'$ and $T = 0.00300$.

Fig. 11. Contourplots of effective interaction on the γ band. The thick line circle around the corner is the Fermi surface γ . (a) For the quasi-particles with parallel spins, $\Gamma_{\gamma\sigma\sigma,\gamma\sigma\sigma}(\mathbf{k}', i\pi T; \mathbf{k}, i\pi T)$. (b) For the quasi-particles with anti-parallel spins, $\Gamma_{\gamma\sigma\bar{\sigma},\gamma\bar{\sigma}\sigma}(\mathbf{k}', i\pi T; \mathbf{k}, i\pi T)$. In both cases, \mathbf{k}' is fixed as pointed by the arrow. The parameters are $U = 3.385$, $U' = 0.500U$, $J = J' = U'$ and $T = 0.00700$.

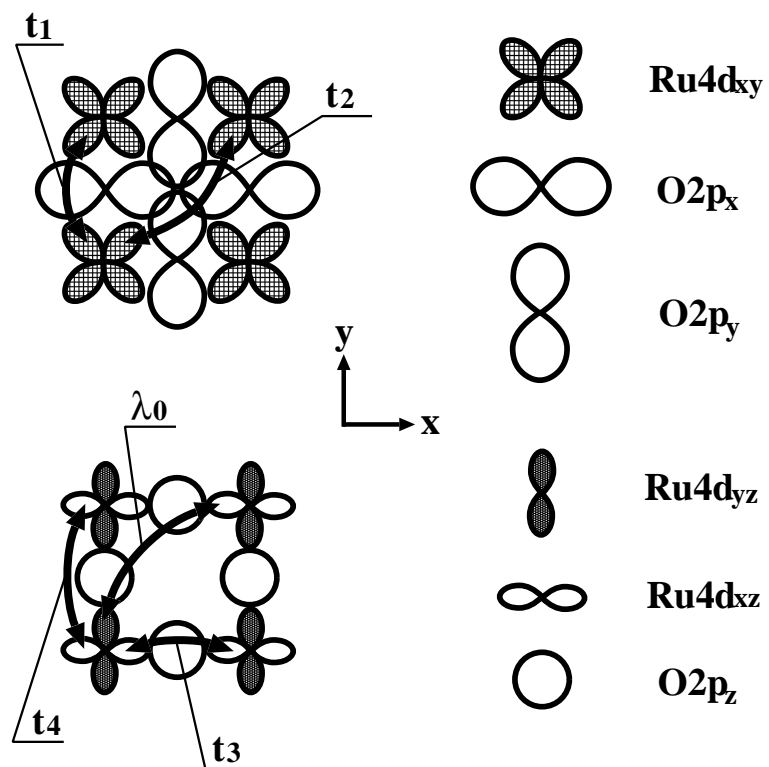


Fig. 1. T. Nomura & K. Yamada

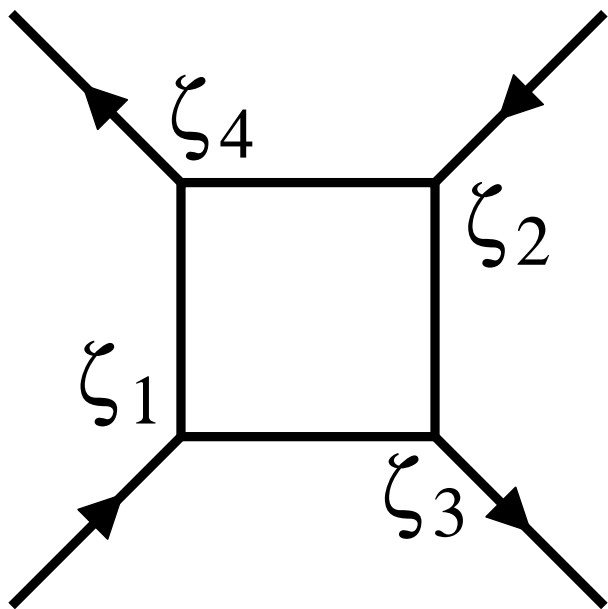
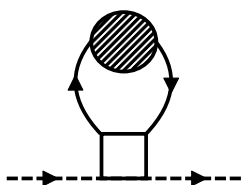
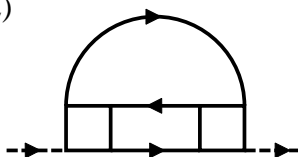


Fig. 2. T. Nomura & K. Yamada

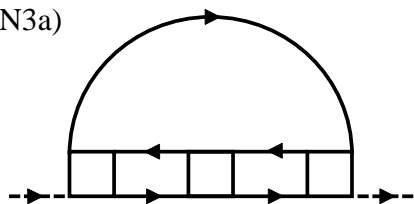
(N1)



(N2)



(N3a)



(N3b)

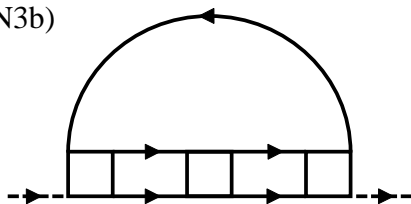


Fig. 3. T. Nomura & K. Yamada

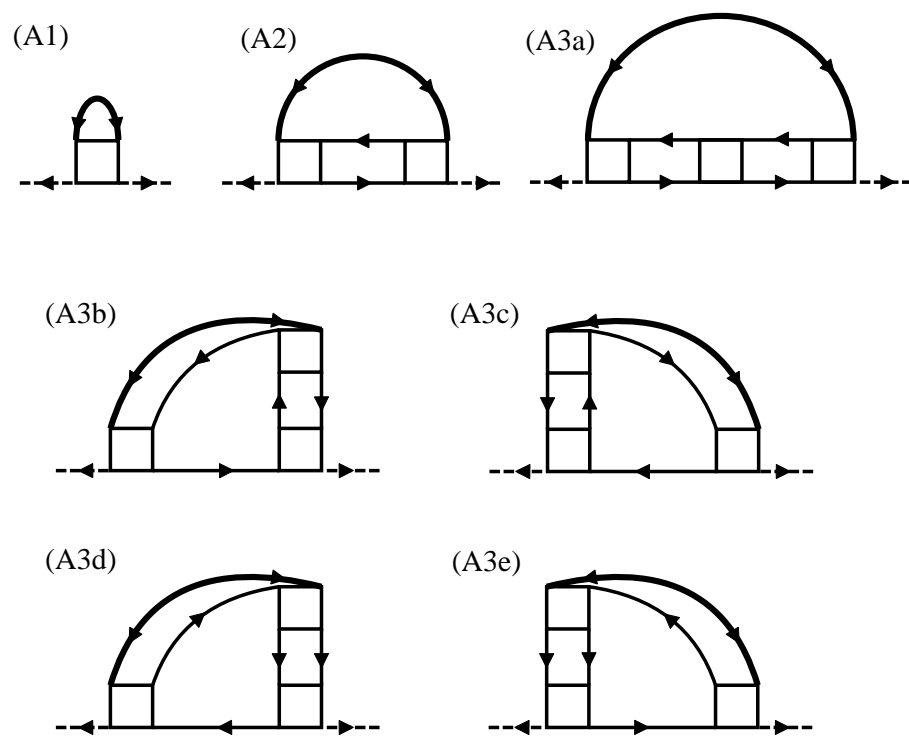


Fig. 4. T. Nomura & K. Yamada

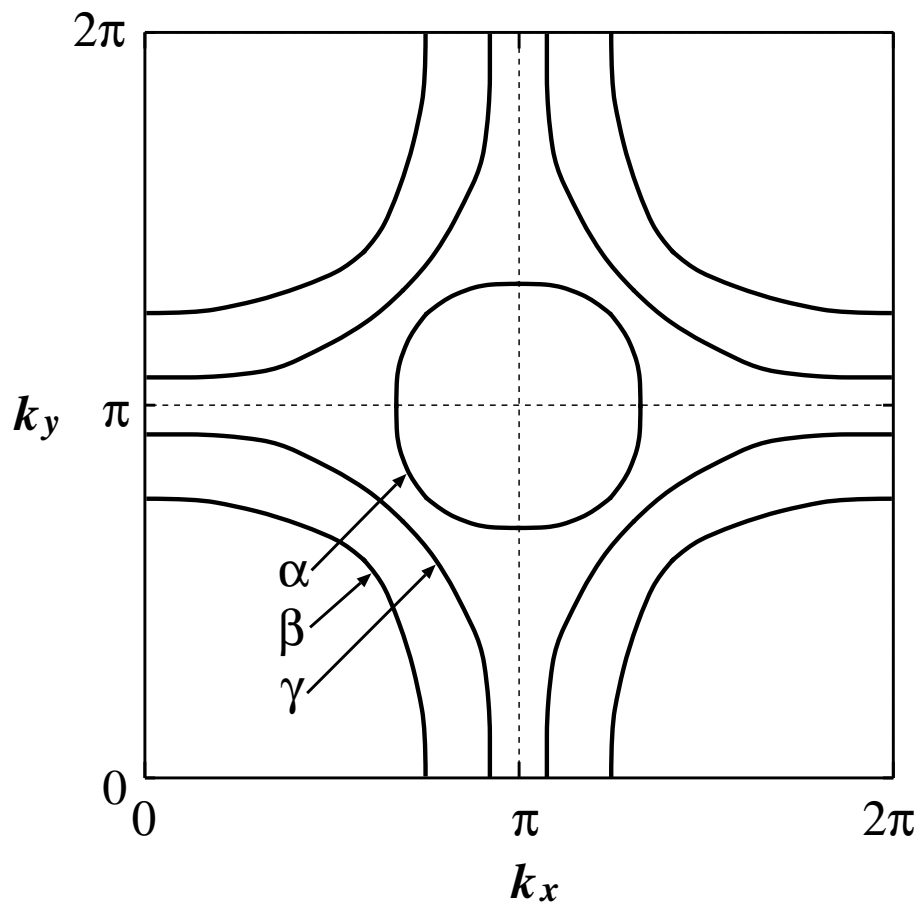


Fig. 5. T. Nomura & K. Yamada

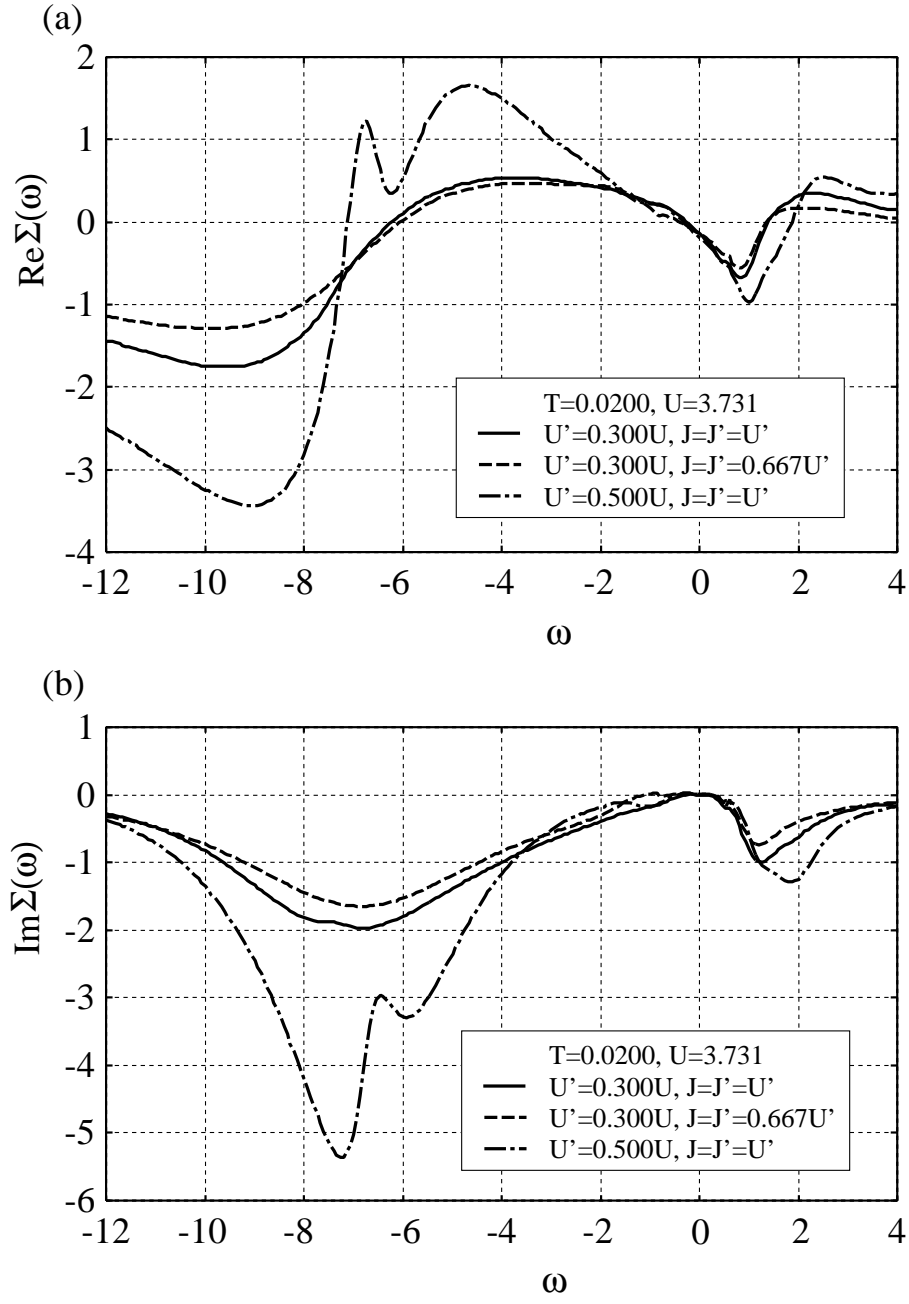


Fig. 6. T. Nomura & K. Yamada

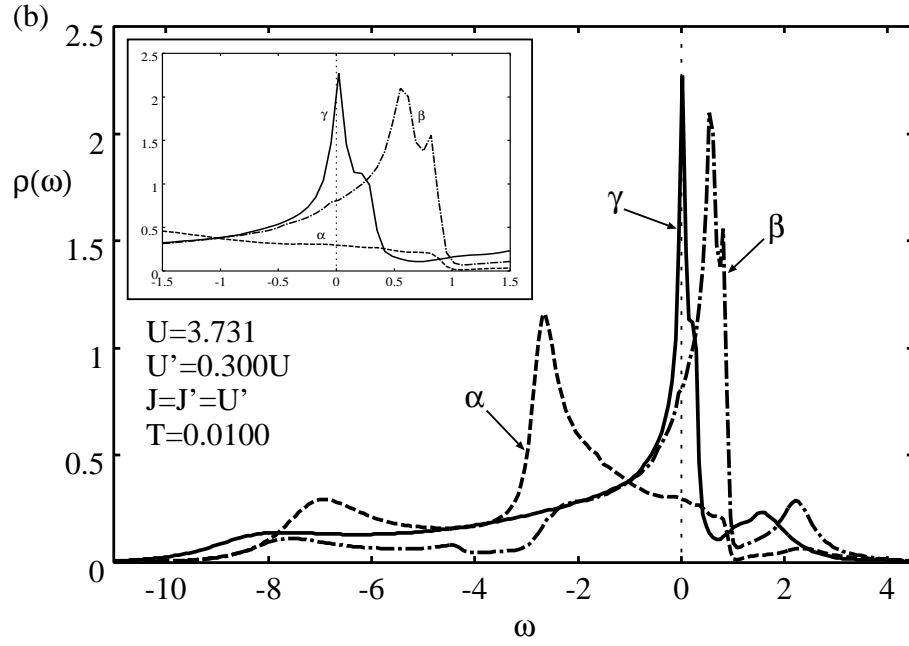
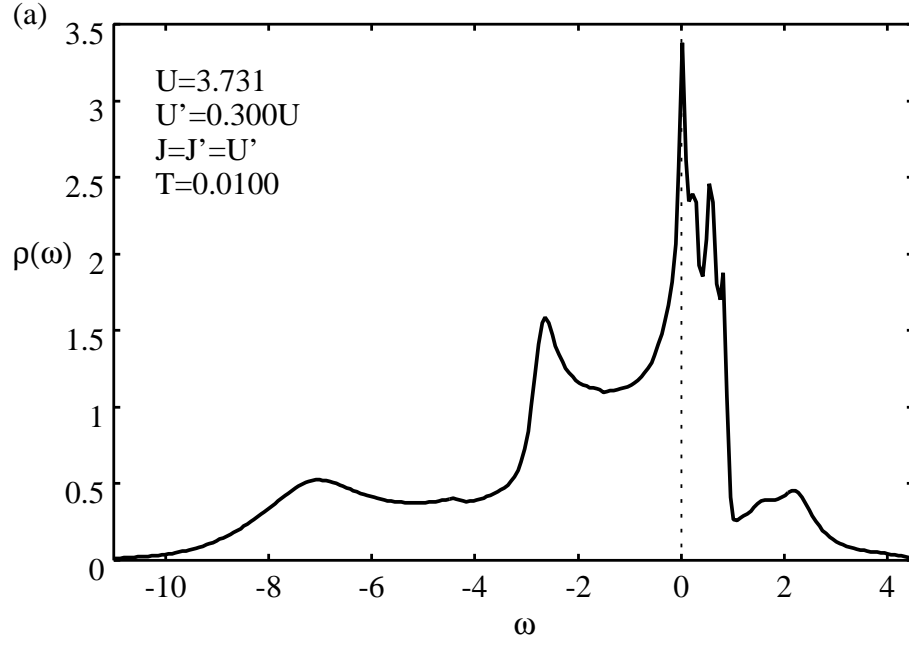


Fig. 7. T. Nomura & K. Yamada

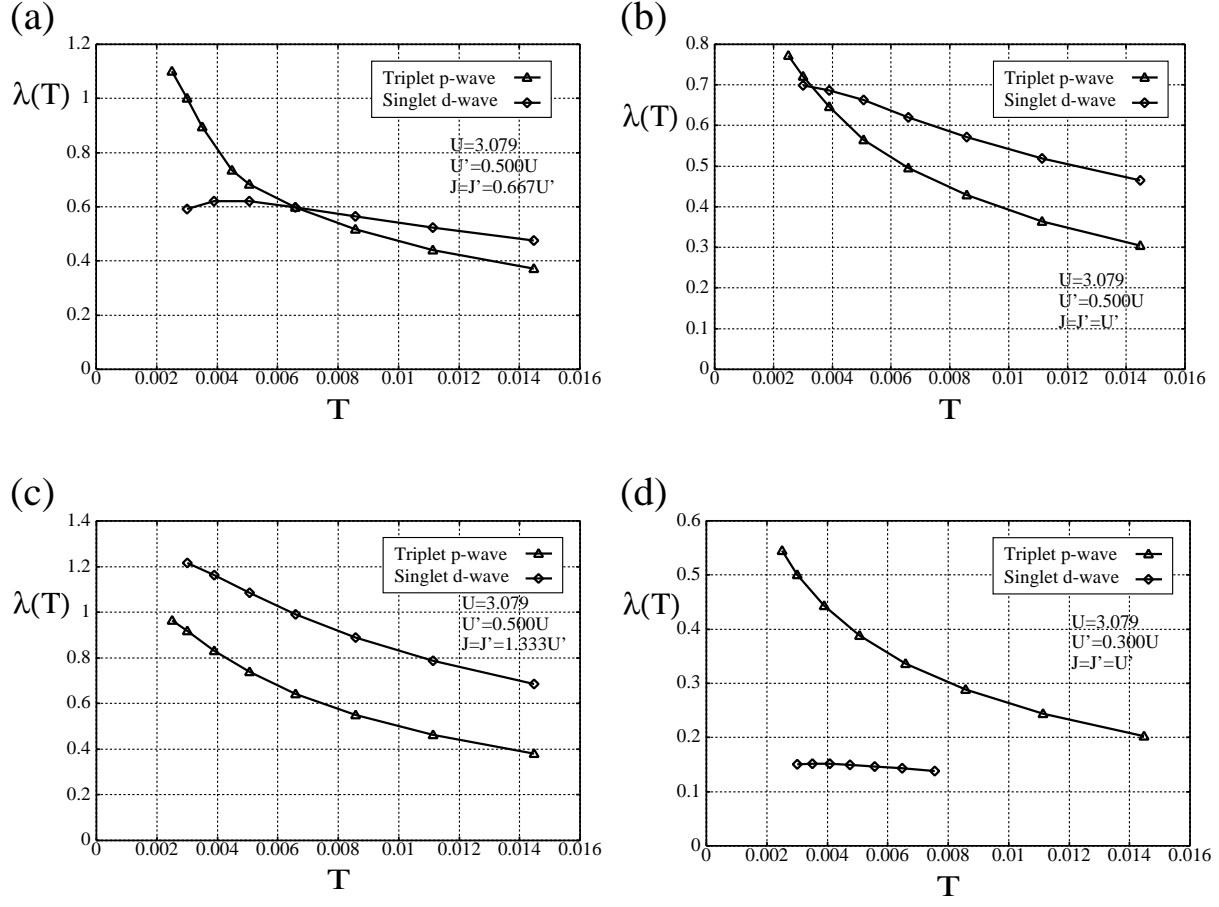


Fig. 8. T. Nomura & K. Yamada

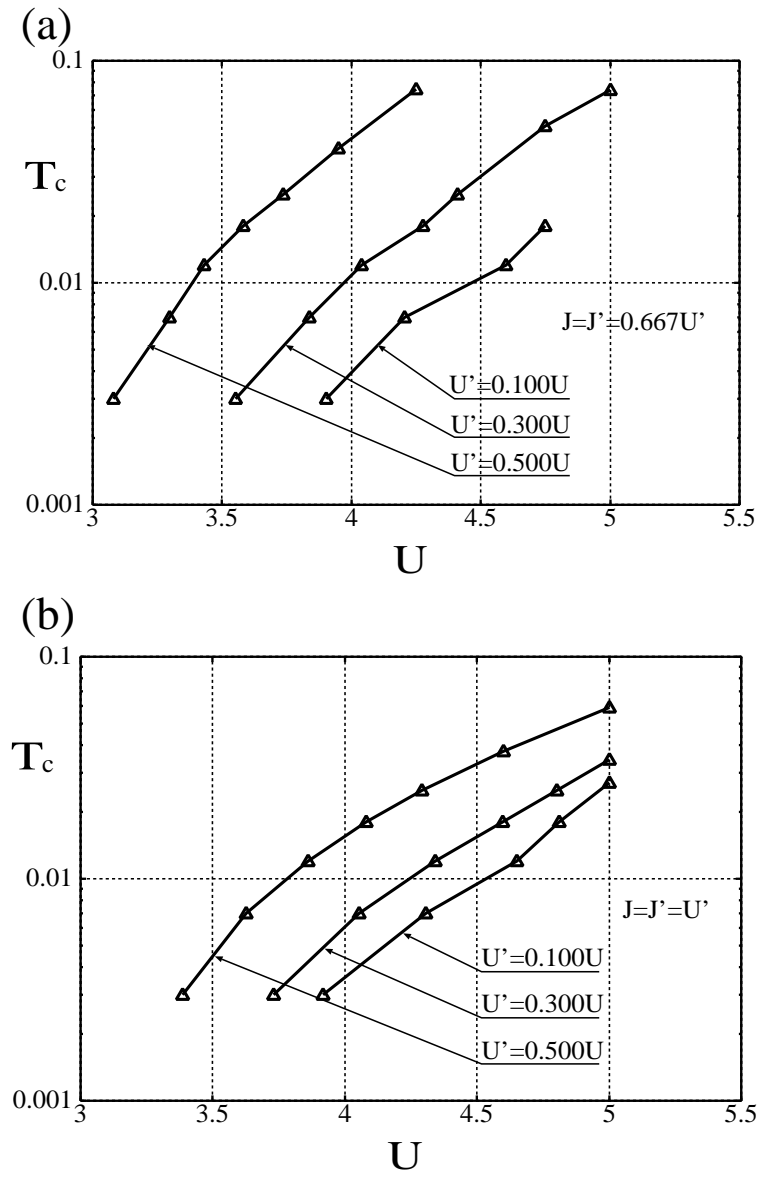


Fig. 9. T. Nomura & K. Yamada

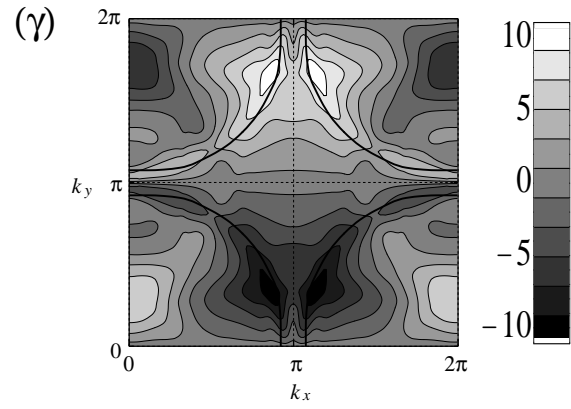
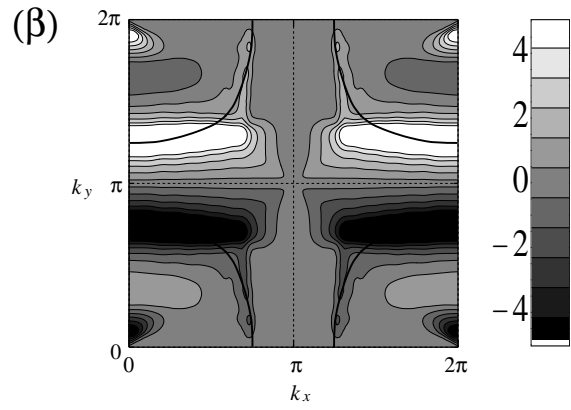
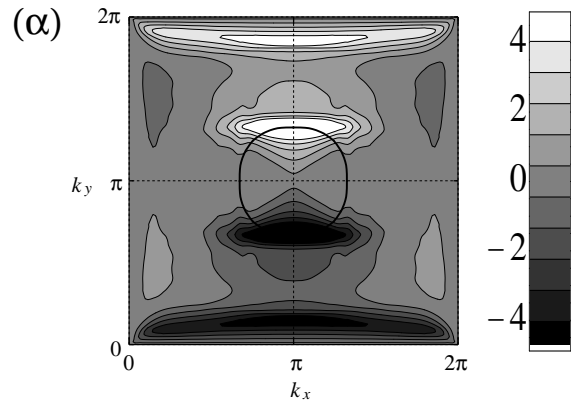


Fig. 10. T. Nomura & K. Yamada

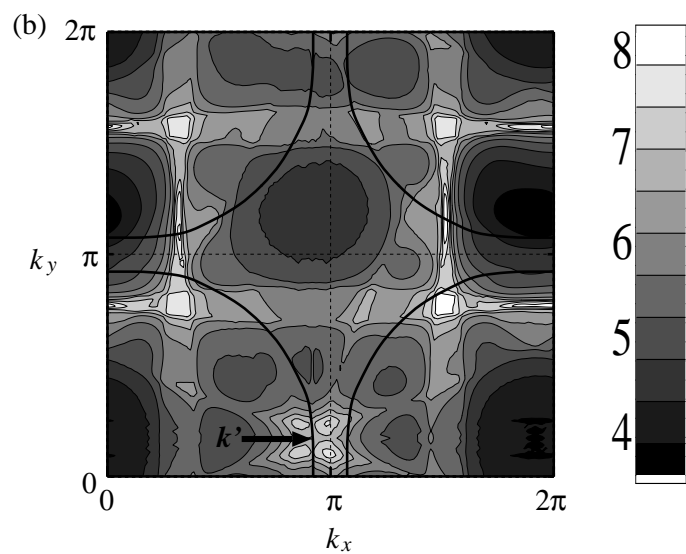
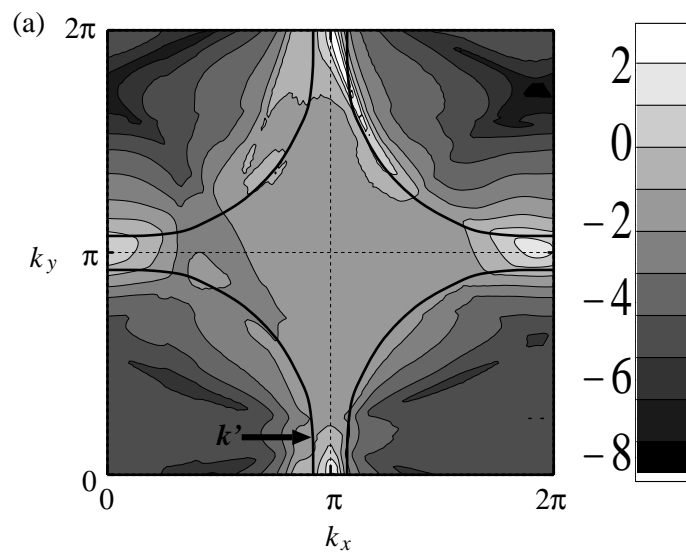


Fig. 11. T. Nomura & K. Yamada